AN INTEGER TONE MAPPING OPERATION FOR HDR IMAGES IN OPENEXR WITH DENORMALIZED NUMBERS

Tatsuya Murofushi[⋆] *Toshiyuki Dobashi*[⋆] *Masahiro Iwahashi*[†] *Hitoshi Kiya*[⋆]

⋆ Tokyo Metropolitan University, Tokyo, 191-0065, Japan
† Nagaoka University of Technology, Niigata, 980-2188, Japan

ABSTRACT

We propose an integer tone mapping operator (TMO) for high dynamic range (HDR) images expressed in a floating-point data format. Two purposes are achieved by the proposed TMO. The first purpose is to implement a TMO with less memory space. The second purpose is to give an important step to realize a fixed-point TMO. The proposed TMO is available for HDR images in the OpenEXR format. The OpenEXR format has two numerical representations (the normalized number and the denormalized number) which are not in other HDR formats such as RGBE. These two numerical representations cause a problem in applying an integer TMO. The proposed method enables us to avoid the problem by using the intermediate format. Moreover, the exponent part and the mantissa part are processed separately as two integer numbers. As a result, an integer TMO with less numerical range is achieved by our method. The experimental results show that the proposed method can generate high-quality low dynamic range (LDR) images with less memory space.

Index Terms— high dynamic range, tone mapping, OpenEXR, denormalized number, integer operation

1. INTRODUCTION

Recently, high dynamic range (HDR) images have been spreading rapidly from the fields of photography and computer graphics, to the other fields such as medical imaging and car-mounted camera. On the contrary, the next generation display devices which can accept so wide range of dynamics of pixel values in HDR images are not popular yet. Therefore, a tone mapping operation (TMO) is important to reduce dynamic range of HDR images so that is can be treated with conventional display devices.

So far, various investigations have been done on TMOs. Most of those were concentrated on finding a tone mapping function suitable for human visual system [1–9]. Recently, some papers dealt with reducing communication cost combining with data compression technologies [10–12]. Unlike those previous studies, this paper discusses on 'resources' of a TMO such as memory space or computational cost for light implementation of tone mapping.

In general, it is important to reduce memory space and computational cost in the image processing, including tone mapping we are discussing here. Heavy demand for computation is continuously increasing, e.g. large variety of color depth, huge size of images and resolution of displaying devices. Therefore, it is still necessary to consider how to implement signal processing under limited resources for economic reason, even though faster machines appear in the future. Especially, a TMO requires heavy resources, since it is generally composed of 'floating point' operations for an HDR data format such as the RGBE [13] and the OpenEXR [14]. Our first purpose is to implement a TMO with less memory space.

An integer TMO in [15] is a tone mapping process implemented in integer input and integer output for HDR images in RGBE format. An integer TMO can reduce the numerical range in calculations. This fact is important for realizing a fixed-point TMO. Based on an integer TMO in [15], a fixed-point TMO for HDR images in RGBE format is proposed in [16]. The fixed-point arithmetic can be executed under limited resources, such as processors without floating-point number processing unit. Moreover, the fixed-point arithmetic is often utilized in the image processing and the embedded system because of the advantages such as the low power consumption, the small circuit size and the high-speed computing [17–19]. However, both integer TMO and fixed-point TMO cannot be applied to HDR images in other HDR formats except the RGBE format. Our second purpose is to construct an integer TMO for the OpenEXR format as an important step to realize a fixed-point TMO.

The small absolute values are treated as denormalized numbers in the OpenEXR format. The denormalized numbers cause a significant damage to resulting low dynamic range (LDR) images when an integer TMO is applied simply. The propose integer TMO avoids this error by introducing of the intermediate format. The experimental results show that the proposed method can generate high-quality LDR images with less memory space.

2. PREPARATION

In this section, we give outlines of a tone mapping operator (TMO) and the OpenEXR format.

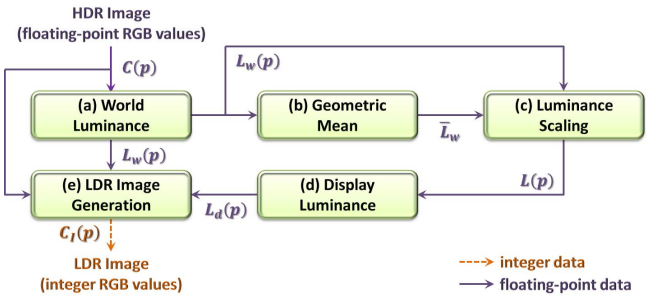

Fig. 1. Photographic Tone Reproduction.

2.1. Tone Mapping Operator

Figure 1 shows "Photographic Tone Reproduction" which is one of the well-known global TMOs [4]. Each process in Fig.1 is described as below.

(a) World Luminance

The input to a TMO for high dynamic range (HDR) images are RGB values $C(p) \in \{R(p), G(p), B(p)\}$ expressed in floating-point numbers. The world luminance $L_w(p)$ of a pixel p is calculated as

$$L_w(p) = 0.27R(p) + 0.67G(p) + 0.06B(p). \quad (1)$$

(b) Geometric Mean

The geometric mean $\overline{L}_w$ of the world luminance $L_w(p)$ is defined as

$$\overline{L}_w = \exp\left(\frac{1}{N}\sum_p \log_e\big(L_w(p)\big)\right), \quad (2)$$

where N is the total number of pixels in the input HDR image. Note that Eq.(2) has singularity due to zero value of $L_w(p)$. It is avoided by introducing a small value in [4]. However, its arbitrariness is not negligible for pixel values in a floating-point format, since its pixel value is also small. Therefore, in this report, we include nonzero values only in the geometric mean.

(c) Scaled Luminance

The scaled luminance $L(p)$ is calculated by

$$L(p) = k \cdot \frac{L_w(p)}{\overline{L}_w}, \quad (3)$$

where $k \in [0, 1]$ is a parameter called "key value."

(d) Display Luminance

The display luminance $L_d(p)$ is computed with a tone mapping function y() as

$$L_d(p) = y(L(p)). \quad (4)$$

The resulting low dynamic range (LDR) image is dependent on the selection of a tone mapping function here. The Reinhard's global operator [4] is specified as

$$y_R(L(p)) = \frac{L(p)}{1 + L(p)}. \quad (5)$$

(e) LDR Image Generation

The RGB values $C_f(p) \in \{R_f(p), G_f(p), B_f(p)\}$ expressed as floating-point numbers are calculated by

$$C_f(p) = L_d(p) \cdot \frac{C(p)}{L_w(p)}. \quad (6)$$

In addition, the 24-bit color RGB values $C_I(p) \in \{R_I(p), G_I(p), B_I(p)\}$ of the resulting LDR image are generated as

$$C_I(p) = \mathrm{round}(C_f(p) \cdot 255), \quad (7)$$

where $\mathrm{round}(x)$ indicates rounding x to the nearest integer value.

In the above procedure, although the resulting LDR image is expressed in the integer data, the data in the middle of calculations are floating-point data with a large dynamic range.

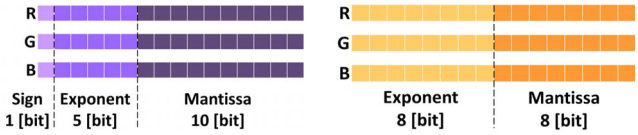

(a) OpenEXR (b) Intermediate Format

Fig. 2. Bit Allocations.

Table 1. The Numerical Restrictions in The OpenEXR.

	Range
Denormalized Number	$0\ ,\ 2^{-24} \sim 2^{-14}$
Normalized Number	$2^{-14} \sim 65504$

2.2. OpenEXR Format

Figure 2(a) shows the bit allocation of the OpenEXR format [1, 14]. The OpenEXR format has the normalized numbers and the denormalized numbers. The range of the normalized numbers is restricted as shown in Table.1. The denormalized numbers can express the small absolute values which cannot be expressed in the normalized numbers. As a result, the OpenEXR format is required to use two different encoding processes and decoding processes [1, 14]. In the decoding process for a normalized number, the relation among a floating-point number F', the exponent part F'_E and the mantissa part F'_M is given as

$$F' = (-1)^{sign} \cdot (1 + F'_M \cdot 2^{-10}) \cdot 2^{F'_E - 15}. \quad (8)$$

In contrast, the relation for a denormalized number is described as

$$F' = (-1)^{sign} \cdot (F'_M \cdot 2^{-10}) \cdot 2^{-14}. \quad (9)$$

In order to generate composite functions for an integer TMO, the unified encoding process and the unified decoding process are required as described later. For this reason, the preprocessing of rounding denormalized numbers to the minimum value which can be expressed as a normalized number is needed. However, this rounding error causes a significant loss in the visual quality of resulting LDR images. The proposed integer TMO will enable us to avoid this error.

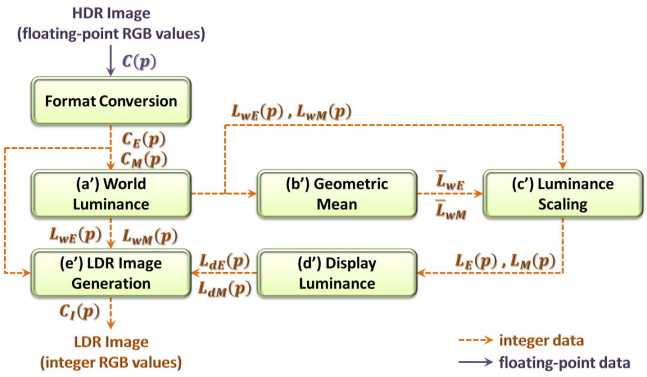

Fig. 3. Proposed Integer TMO.

Note that only the case of positive values is taken into consideration in this paper. Although the OpenEXR format can also express negative values, the impact of the negative values is small since a pixel value is a positive value in general.

3. PROPOSED INTEGER TMO

In this section, we consider an integer TMO for HDR images in the OpenEXR format. The proposed integer TMO is summarized as shown in Fig.3.

3.1. Intermediate Format

The intermediate format shown in Fig.2(b) is utilized to avoid a significant damage due to the use of denormalized numbers. Note that any denormalized numbers in the OpenEXR format are included in the range of the intermediate format, although they are not included in that of normalized numbers. In the intermediate format, the relation among a floating-point number F, the exponent part F_E and the mantissa part F_M is defined as

$$F = (F_M + 0.5) \cdot 2^{F_E - 136}. \tag{10}$$

The converse relation is given as

$$F_E = \lceil \log_2 F + 128 \rceil, \tag{11}$$

$$F_M = \lfloor F \cdot 2^{136 - F_E} \rfloor, \tag{12}$$

where $\lceil x \rceil$ rounds x up to the nearest integer, and $\lfloor x \rfloor$ rounds x down to the nearest integer.

3.2. Integer TMO for OpenEXR

In this paper, the integer TMO is defined as the TMO which is implemented in integer input and integer output. The integer TMO is realized by replacing each tone mapping process with a new process as the composite function in Fig.4. In the proposed integer TMO, the numerical range in the tone mapping process can be significantly reduced because the exponent part and the mantissa part are separated as two integer numbers.

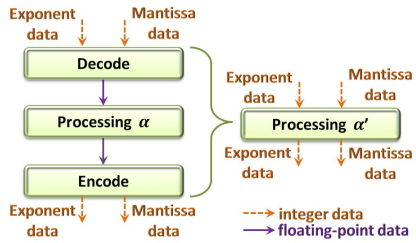

Fig. 4. Generation of Composite Function.

The proposed integer TMO converts RGB values $C(p)$ expressed as the OpenEXR format into the intermediate format data specified in Fig.2(b) at the first stage. The exponent part $C_E(p) \in \{R_E(p), G_E(p), B_E(p)\}$ and the mantissa part $C_M(p) \in \{R_M(p), G_M(p), B_M(p)\}$ are converted as

$$C_E(p) = \lceil \log_2 C(p) + 128 \rceil, \tag{13}$$

$$C_M(p) = \lfloor C(p) \cdot 2^{136 - C_E} \rfloor. \tag{14}$$

Each process in Fig.3 is computed as follows.

(a') World Luminance

The exponent part $L_{wE}(p)$ and the mantissa part $L_{wM}(p)$ of the world luminance $L_w(p)$ are given as

$$L_{wE}(p) = \lceil \log_2 L_{wt}(p) - 8 \rceil, \tag{15}$$

$$L_{wM}(p) = \lfloor L_{wt}(p) \cdot 2^{-L_{wE}(p)} \rfloor, \tag{16}$$

$$\begin{aligned} L_{wt}(p) = {} & 0.27(R_M(p) + 0.5) \cdot 2^{R_E(p)} + \\ & 0.67(G_M(p) + 0.5) \cdot 2^{G_E(p)} + \\ & 0.06(B_M(p) + 0.5) \cdot 2^{B_E(p)}, \end{aligned} \tag{17}$$

where $L_{wt}(p)$ is calculated using only nonzero RGB channels. $L_{wt}(p)$ is defined as zero value at the pixel p in which the all RGB channels at p have a value of zero. Other values in subsequent calculations are set to zero as well as in $L_{wt}(p)$.

(b') Geometric Mean

The exponent part $\overline{L}_{wE}$ and the mantissa part $\overline{L}_{wM}$ of the geometric mean $\overline{L}_w$ are derived as

$$\overline{L}_{wE} = \lceil L_{wt1} + L_{wt2} + 128 \rceil, \tag{18}$$

$$\overline{L}_{wM} = \lceil 2^{L_{wt1} + L_{wt2} - \overline{L}_{wE} + 136} \rfloor, \tag{19}$$

$$\overline{L}_{wt1} = \frac{1}{N} \sum_p \log_2 (L_{wM}(p) + 0.5), \tag{20}$$

$$\overline{L}_{wt2} = \frac{1}{N} \sum_p (L_{wE}(p) - 136). \tag{21}$$

(c') Scaled Luminance

The exponent part $L_E(p)$ and the mantissa part $L_M(p)$ of the scaled luminance $L(p)$ is calculated by

$$L_E(p) = \lceil \log_2 L_t(p) + L_{wE}(p) - \overline{L}_{wE} + 128 \rceil, \tag{22}$$

$$L_M(p) = \lfloor L_t(p) \cdot 2^{L_{wE}(p) - L_E(p) - \overline{L}_{wE} + 136} \rfloor, \tag{23}$$

$$L_t(p) = k \cdot \frac{L_{wM}(p) + 0.5}{\overline{L}_{wM} + 0.5}. \quad (24)$$

(d') Display Luminance

The exponent part $L_{dE}(p)$ and mantissa part $L_{dM}(p)$ of the display luminance $L_d(p)$ is computed with a tone mapping function. This process depends on the used tone mapping function. When the function in Eq.(5) is used, the equation is given as

$$L_{dE}(p) = \lceil \log_2 L_{dt}(p) + 128 \rceil, \quad (25)$$

$$L_{dM}(p) = \lfloor L_{dt}(p) \cdot 2^{136 - L_{dE}(p)} \rfloor, \quad (26)$$

$$L_{dt}(p) = \frac{L_M(p) + 0.5}{L_M(p) + 0.5 + 2^{136 - L_E(p)}}. \quad (27)$$

(e') LDR Image Generation

The 24-bit color RGB values $C_I(p)$ of the resulting LDR image are obtained by

$$C_I(p) = \text{round}\{C_{It}(p) \cdot 2^{C_E(p) + L_{dE}(p) - L_{wE}(p) - 136} \cdot 255\}, \quad (28)$$

$$C_{It}(p) = \frac{(L_{dM}(p) + 0.5)(C_M(p) + 0.5)}{L_{wM}(p) + 0.5}. \quad (29)$$

In the above procedure, all input and output of tone mapping process can be realized as two integers corresponding to the exponent part and the mantissa part of each data.

Two kinds of errors arise due to the use of the proposed integer TMO with the intermediate format. The first error arises in the format conversion from OpenEXR format. The second error is attributed to rounding calculation results to two integers. The following section shows that these errors are too small to affect the subjective visual quality.

4. EXPERIMENTAL RESULTS

Two integer TMOs, one utilizes the OpenEXR format directly and the other utilizes the intermediate format, have been considered in this paper. In this section, it is shown that the integer TMO with intermediate format offers high-quality LDR images equivalent to the results by the conventional method [4] with floating-point numbers. The 42 HDR images in the OpenEXR format was utilized in our experiment. All floating-point values were computed and stored in the double-precision floating-point format. The Reinhard's global operator [4] in Eq.(5) was used as an example of tone mapping functions. Moreover, the memory space comparison between the integer TMO with the intermediate format and conventional method was also performed.

4.1. PSNR Result

The integer TMO without the intermediate format and the integer TMO with it were compared. Table.2 shows the peak signal-to-noise ratio (PSNR) results and the maximum error of RGB pixel values. The PSNR between the LDR image generated by the two integer TMOs and that generated by the conventional method was evaluated. The minimum PSNR with the intermediate format is 49.0 dB, and it shows the better result than 33.8 dB attributed to the directly use of the OpenEXR format. The maximum error of RGB pixel values with the intermediate format also shows the sharply better result. The rounding errors of denormalized numbers in the OpenEXR format worsens the quality of resulting LDR images. In contrast, since rounding the denormalized numbers is not necessary, the integer TMO with the intermediate format can generate high-quality LDR images from all input HDR images. Note that the intermediate format assigns fewer bits to the mantissa part than the OpenEXR format even though it can express the larger numerical range.

Table 2. PSNR and Pixel Values Error.

	without Intermediate	with Intermediate
Minimum PSNR [dB]	33.8	49.0
Maximum pixel values error	47	3

Table 3. MEMORY SPACE.

Data	Conventional	Proposed
HDR RGB Values	192 bit/pixel	48 bit/pixel
World Luminance	64 bit/pixel	16 bit/pixel
Geometric Mean	64 bit	16 bit
Scaled Luminance	64 bit/pixel	16 bit/pixel
Display Luminance	64 bit/pixel	16 bit/pixel
LDR RGB Values	24 bit/pixel	24 bit/pixel

4.2. Comparison of Memory Space

Table.3 shows the memory space in each of the conventional method with floating-point numbers and the proposed integer TMO with the intermediate format. It indicates that the proposed integer TMO significantly reduces memory resources comparing to the conventional method. The memory resources to store data are reduced from 192 to 48 bit/pixel (25 %) at maximum by the proposed integer TMO.

5. CONCLUSION

In this paper, we proposed an integer TMO which is implemented in integer input and integer output for HDR images in the OpenEXR format. The integer TMO processes the exponent part and the mantissa part separately as two integer numbers; therefore, the numerical range in the tone mapping process is greatly reduced. The intermediate format enables us to avoid a significant damage due to the use of denormalized numbers in the OpenEXR format. As a result, it was confirmed that the integer TMO with the intermediate format offers high-quality LDR images equivalent to the results by the conventional method with floating-point numbers. It was also verified that the memory space are reduced to from 192 to 48 bit/pixel at maximum by the proposed integer TMO.

6. REFERENCES

[1] E. Reinhard, G. Ward, S. Pattanaik, P. Debevec, W. Heidrich and K. Myszkowski, *High Dynamic Range Imaging : Acquisition, Display, and Image-Based Lighting.* second edition, San Francisco, CA, USA: Morgan Kaufmann Publishers, 2010.

[2] J. Duan, and G. Qiu, "Fast Tone Mapping for High Dynamic Range Images," *Proc. IEEE ICPR*, Vol. 2, pp. 847-850, Aug. 2004.

[3] A. Koz, and F. Dufaux, "Optimized Tone Mapping with LDR Image Quality Constraint for Backward-Compatible High Dynamic Range Image and Video Coding," *Proc. IEEE ICIP*, pp. 1762-1766, Sept. 2013.

[4] E. Reinhard, M. Stark, P. Shirley, and J. Ferwerda, "Photographic Tone Reproduction for Digital Images," *ACM Trans. on Graphics*, Vol. 21, pp. 267-276, July. 2002.

[5] F. Drago, K. Myszkowski, T. Annen, and N. Chiba, "Adaptive Logarithmic Mapping for Displaying High Contrast Scenes," *Comput. Graph. Forum*, Vol.22, pp. 419-426, 2003.

[6] S. N. Pattanaik, J. Tumblin, H. Yee, and D. P. Greenberg, "Time-Dependent Visual Adaptation for Fast Realistic Image Display," *Proc. ACM SIGGRAPH*, pp. 47-54, July. 2000.

[7] K. Chiu, C. H. Shirley, P. Shirley, S. Swamy, C. Wang and K. Zimmerman, "Spatially Nonuniform Scaling Functions for High Contrast Images," *Proc. Graphics Interface*, pp. 245-253, May. 1993.

[8] F. Durand and J. Dorsey, "Fast Bilateral Filtering for the Display of High-Dynamic-Range Images," *ACM Trans. on Graphics*, Vol. 21, pp. 257-266, July. 2002.

[9] R. Fattal, D. Lischinski, and M. Werman, "Gradient Domain High Dynamic Range Compression," *ACM Trans. on Graphics*, Vol. 21, pp. 249-256, July. 2002.

[10] M. Iwahashi and H. Kiya, "Efficient Lossless Bit Depth Scalable Coding for HDR Images," *Proc. APSIPA ASC*, no.OS.49-IVM, 17-5, Dec. 2012.

[11] M. Iwahashi and H. Kiya, "Two Layer Lossless Coding of HDR Images," *Proc. IEEE ICASSP*, pp. 1340-1344, May. 2013.

[12] R. Xu, S. N. Pattanaik, and C. E. Hughes, "High-Dynamic-Range Still Image Encoding in JPEG2000," *Proc. IEEE CGA*, Vol. 25, No. 6, pp. 57-64, Nov. 2005.

[13] G. Ward, "Real Pixels," *Graphics Gems 2.*, pp. 80-83, San Diego, CA, USA: Academic Press, 1992.

[14] F. Kainz, R. Bogart, and D. Hess, "The Openexr Image File Format," *ACM SIGGRAPH '03 Technical Sketches*, 2003.

[15] T. Murofushi, M. Iwahashi, and H. Kiya, "An Integer Tone Mapping Operation for HDR Images Expressed in Floating Point Data," *Proc. IEEE ICASSP*, pp. 2479-2483, May. 2013.

[16] T. Dobashi, T. Murofushi, M. Iwahashi, and H. Kiya, "A Fixed-Point Tone Mapping Operation for HDR Images in the RGBE Format," *Proc. APSIPA ASC*, no.OS.37-IVM, 16-4, Nov. 2013.

[17] T. Viitanen, P. Jaaskelainen, O. Esko, and J. Takala, "Simplified Floating-point Division and Square Root," *Proc. IEEE ICASSP*, pp. 2707-2711, May. 2013.

[18] C. H. Lampert, and O. Wirjadi, "Anisotropic Gaussian Filtering Using Fixed Point Arithmetic," *Proc. IEEE ICIP*, pp. 1565-1568, Oct. 2006.

[19] K. J. Hass, "Synthesizing Optimal Fixed-Point Arithmetic for Embedded Signal Processing," *Proc. IEEE MWSCAS*, pp. 61-64, Aug. 2010.